*H. Uematsu**, *T. Natsuume*, *S. Tanoue*, *Y. Iemoto*

Department of Frontier Fiber Technology and Science, University of Fukui, Fukui, Japan

Effect of Flow Induced Orientation of Carbon Nanotubes on the Capillary Extrusion Behavior of Low-Density Polyethylene

The effect of carbon nanotubes (CNTs) on the capillary extrusion behavior of low-density polyethylene (PE) was investigated. From the linear viscoelasticity and the morphology observation, it was found that the CNTs were well dispersed throughout the PE matrix and our system belonged to the semi-dilute regime. The strain hardening, which quantifies the extension of the PE chain, decreased by presence of CNTs in the uniaxial elongational deformation. In contrast, the normal stress difference was almost unaffected by CNTs in the shear deformation. The capillary extrusion behavior revealed that swell ratio decreased with increasing the CNT content although melt fracture was promoted. We summarize that the suppression of swell and promotion of melt fracture are attributable to the orientation of CNTs.

1 Introduction

The appearance and properties of the materials shaped in polymer or food extrusion processes depend on the extrusion conditions. At low extrusion rates, the diameter of the extruded material exceeds that of the die. This behavior, called die swell or Barus effect, is one of the most important viscoelastic responses of polymer melts because it largely determines the size and shape of the extruded materials. As is well known, the diameter of the extrudate is bigger than that of the die because of the elastic recovery at the die exit (Tanoue and Iemoto, 1999; Mu and Zhao, 2010). However, relatively high extrusion rates often induce flow instabilities, which manifest as surface failures and volume distortions. Visually, these defects resemble orange peel, sharkskin, screw-threaded, helical, or gross (chaotic) form. Volume distortions are usually referred to as melt fractures. Flow instabilities cause surface and shape irregularities, which reduce the transparency and mechanical properties of the extruded materials. Hence, the mechanisms of flow instabilities have been investigated over many years. Melt factures are easily developed in long-chain branched polymer systems with high molecular weight components (Goutille et al., 2003; Yamaguchi et al., 2003). The recognized source of melt facture is flow instability at the die entrance (Wassner et al., 1999; Nigen et al., 2003). Meller et al. (2002) elucidated the development of volume distortion by investigating how the extensional stress at the die entrance depends on the shear stress at the die wall. Thus, we suggest that the elastic component might control the swelling phenomenon and flow instability in an extruded product. However, reducing the elastic component to remove swelling and flow instability would also degrade the properties (e. g., strength) of the extruded materials at room temperature. Therefore, from an industrial perspective, methods that control the extrusion behavior while preserving the elastic component are required.

To expand the functionality of products, polymeric materials are often combined with other materials. Nano-size additives such as clay and carbon nanotubes (CNTs) can improve the mechanical, electrical, and thermal properties of materials (Ma et al., 2010; Dalir et al., 2012). Understanding the extrusion behavior of the composite is necessary in actual polymer extrusion processing, because the swelling phenomenon and flow stability directly affect the product processability. Addition of clay (Chen et al., 2005; Muksing et al., 2008) and CNT (Kharchenko et al., 2004) was reported to reduce the swell, most likely by reducing the elastic properties of the material. Adding carbon fiber with a high aspect ratio increases the swell of polymer at high extrusion rates, but reduces it at low extrusion rates (Hausnerova et al., 2006). Composites with high entanglement and/or large contact among concentrated rigid fillers have been frequently reported. However, the swell behavior of molten polymers containing highly dispersed rigid fillers has been largely neglected. Previously, we reported the effect of highly dispersed CNTs on the extrusion behavior of dense polyethylene (Uematsu et al., 2013). In shear and elongational rheology studies, we demonstrated that the chain extension in CNT-supplemented polymer is reduced by the decreased swell and the inhibition of helical extrudates (regular volume distortion). Therefore, it was suggested that small amounts of CNT will suppress the swell and flow instability without compromising the shear viscosity. On the other hand, a rigid fiber famously orients in the accelerated and/or decelerated flow field (Ausias, 1994; Chiba and Nakamura, 1998). However, the extrusion behavior has been hardly investigated

* Mail address: Hideyuki Uematsu, Department of Frontier Fiber Technology and Science, University of Fukui, 3-9-1, Bunkyo, Fukui-shi, Fukui 910-8507, Japan
E-mail: uematsu@matse.u-fukui.ac.jp

from a view point of the orientation of rigid fiber at die exit. In the present paper, we investigate whether CNT can moderate the extrusion behavior of long branched chain polymers in terms of the orientation of rigid fibers.

2 Experimental Procedure

2.1 Materials

The polymer used in this study was a low-density polyethylene (PE) (LJ401, Japan Polyethylene Corporation, Japan) with a density of 0.92 g/cm^3, a melt index of 1.5 g/10 min, M_w = 95.5 kg/mol, and a polydispersity index of 5.13. CNT with a density of 2.1 g/cm^3 consisted of vapor-grown carbon fibers manufactured by Showa Denko K. K., Japan. The average diameter and length of the CNTs were 150 nm and 6 μm, respectively. The PE and CNTs were compounded in a co-rotating twin screw extruder (S1 KRC kneader, Kurimoto Ltd., Japan), and the mixed samples were pelletized. The screw diameter and length/diameter ratio were 25 mm and 10.2, respectively. The barrel temperature and screw rotation speed were respectively set to 200 °C and 150 min^{-1}. The CNT content was varied from 0 to 5 wt%. In this paper, the composite containing 5 wt% CNT is denoted as PE/CNT5 (composites containing other CNT contents are defined similarly). PE/CNT composite pellets were compression-molded into disks (diameter = 25 mm and thickness = 0.5 to 1.0 mm) or rectangular bars (length = 15 mm; width = 5 mm; thickness = 0.5 mm). The disks and bars were subjected to shear rheological testing and uniaxial elongational viscosity measurements, respectively. The composite pellets were melted in a mold maintained at 200 °C for 5 min. Next, the samples were shaped under a pressure of 20 MPa, which was gradually applied and maintained for 5 min. The molded samples were cooled at room temperature for 10 min. The capillary extrusion behavior of the samples was investigated.

2.2 Measurements

Rheological measurements of PE/CNT were conducted with a rotational rheometer (MCR, Anton Paar) at 200 °C. Frequency (ω) sweeps were applied to parallel plates of diameter 25 mm separated by approximately 0.5 mm. The ω dependencies of the storage and loss moduli (G′ and G″ respectively) were measured in the ω range of 0.1 to 100 rad/s. The strain was varied from 0.01 to 0.2, within the linear viscoelastic criterion of the PE composite. The steady shear viscosity η_s was measured at 200 °C by using parallel plates geometry in the transient shear flow mode, varying the shear rate from 0.003 to 0.01 s^{-1}. Creep and creep-recovery experiments were performed at 200 °C at shear stresses of 5 and 10 Pa with parallel plates geometry. A cone and plate geometry with a plate diameter of 25 mm and cone angle of 2° was used for measurement of the normal stress difference N_1 in the shear rate from 0.1 to 10 s^{-1}. The uniaxial elongational viscosity η_E was measured at a constant strain rate in the transient uniaxial elongational deformation mode at 200 °C. The true strain rate $\dot{\varepsilon}$ was applied by a analyzing the width versus time obtained by a video camera. All rheological measurements were performed under nitrogen atmosphere.

To evaluate the appearance of the extrudates, the capillary extrusion behavior was measured at 200 °C by the capillary rheometer (CFT-500D, Simadzu Corporation). In these tests, the barrel diameter was 11 mm, and the L/D of the circular die was 10/1. The pressure drop ΔP between the entrance and exit of the capillary die was evaluated by varying the L/D of the circular die as 1/1, 2/1, and 10/1. The entrance angle of the circular die was 180°. After melting the PE/CNT pellets in the barrel for 10 min, the volumetric flow rate of the composite was measured under various constant loads (from 98 to 980 N). The apparent shear rate and apparent shear stress on the circular die wall were calculated from the volumetric flow rate and load, respectively.

The morphology of the samples was observed using scanning electron microscopy SEM (S-3400 N, Hitachi High-Technologies Corporation) to investigate the dispersed state of the CNTs in the matrix. All samples were coated with platinum for 5 min in order to make the samples conductive. SEM analysis was performed under the standard high vacuum mode and the voltage was kept at 15 kV.

3 Results and Discussion

3.1 Rheological Response under Shear and Elongational Flow

The effect of CNT on the simple rheological behavior under shear and elongational deformation of the polymeric material is important, because it reflects the complex flow history of the extrusion process. Therefore, we first evaluated the dispersion of CNTs in the molten state by investigating the dynamic viscoelasticity of molten PE/CNT. The storage modulus G′ and loss modulus G″ of PE/CNT as a function of frequency are plotted in Fig. 1. G′ and G″ of PE slightly increased with CNT content in the entire frequency range. The slopes of G′ and G″ were similarly independent of the CNT content and approached 2 and 1, respectively, in the low-frequency limit. The plateau G′ originated from a percolated network of CNTs was not seen in our system. In order to confirm the dispersion state of CNTs in the PE matrix, the morphology was investigated by scanning electron microscopy SEM. Figure 2 shows a cross sectional surface of the specimens of rheological tests. CNTs were well dispersed and isolated from each other in the PE matrix regardless of CNT content. A portion of CNT had a length of around 5 μm and the majority of CNT had a length of around 1 μm. Previously, we found that the average length of the same CNTs in a polycarbonate matrix decreased by 60 % to 70 % after mixing with the same co-rotating twin screw extruder, irrespective of the CNT content (Nithikarnjanatharn et al., 2012). It would be safe to say that the average length of CNT decreased less than 50 % in comparison with the value mixing (average length of 6 μm).

In suspensions of rod-like fillers with diameter d and length L in a polymer matrix, different concentration regimes can be distinguished by the number v of rods per volume element as $v = 4\,\phi/(\pi L d^2)$, where ϕ is the volume fraction of rods (Larson, 1999). The interactions between the rods can be neglected in the dilute regime ($v < 1/L^3$). In the semi-dilute regime ($1/L^3 < v < 1/(dL^2)$), the interaction between the rods is relevant (Schmid et al., 2000; Switzer and Klingenberg, 2003). The

dense network of rods exists and the free motion of rods is strongly suppressed in concentrated regime ($v > 1/(dL^2)$) (Ferec et al., 2009; Handge et al., 2011; Vega et al., 2014). In our system, the ϕ of CNT ranges in the interval between 0.3 vol% and 2.2 vol% from these densities and weight ratio ϕ_w. Assuming a CNT length of 3 μm after mixing, v of CNT ranges between 0.08 μm^{-3} to 0.41 μm^{-3}. The values of $1/L^3$ and $1/(dL^2)$ were calculated as 0.037 μm^{-3} and 0.74 μm^{-3}, respectively. Therefore, our system containing CNTs ranging from 1 wt% to 5 wt% belongs to semi-dilute regime. If the length of CNT decreased by 20% after mixing, these samples are situated in the semi-dilute regime. It is a reasonable result that the plateau G′ based on the percolated network of CNTs was not shown in our system (Fig. 1). However, the delayed dynamics seems not to be significant in our sample. To confirm the terminal region for chain relaxation in these samples, the creep test was performed at low enough value of shear stress for long creep time. Figure 3A shows the creep compliance J of PE and PE/CNT5 at shear stresses of 5 Pa and 10 Pa. The results for J are within the linear viscoelastic region because J did not depend on the shear stress and the slope of J was 1 in the long time region. In other words, the terminal region for chain relaxation is reached for these samples. From these results, it is possible to obtain the value of zero-shear viscosity η_0 as

$$\eta_0 = \lim_{t\to\infty} t/J(t). \quad (1)$$

The η_0 calculated from J, shear viscosity η_s measured in the steady shear flow mode and complex viscosities η^* of PE and PE/CNT5 are plotted as a function of strain rate $\dot{\gamma}$ and dynamic frequency ω in Fig. 3B. The η_0 of PE increased 1.2 times by the presence of 5 wt% of CNT although the relaxation time hardly changed. Usually, in small-amplitude oscillatory shear, η^* versus dynamic frequency ω is numerically equal to η_s versus $\dot{\gamma}$ according to the empirical Cox–Merz rule (Cox and Merz, 1958) in homogeneous systems. However, the Cox–Merz rule holds irrespective of the CNT in our inhomogeneous system. In a previous report, the viscosity and the terminal relaxation time of the polymer matrix hardly changed in spite of concentrated regime of CNTs in a matrix with a high polydispersity index such as long branched chain matrix (Vega et al., 2014). Vega et al. (2014) also suggest that it will not be possible to detect the CNTs network if the relaxation time of the matrix is high enough. Therefore, the delayed dynamics might be screened in our system because the matrix has a long branched chain. The important part of these results is that the CNTs are well dispersed in the matrix and our system belongs to the semi-dilute regime.

Second, we investigated the elongational rheology of PE/CNT. Panels (a) and (b) of Fig. 4 show the uniaxial elongational viscosity η_E^+ of PE and PE/CNT5, respectively, measured at 200 °C under various strain rates $\dot{\varepsilon}$. The solid lines denote $3\eta_s^+$ measured by a rotational rheometer at different times

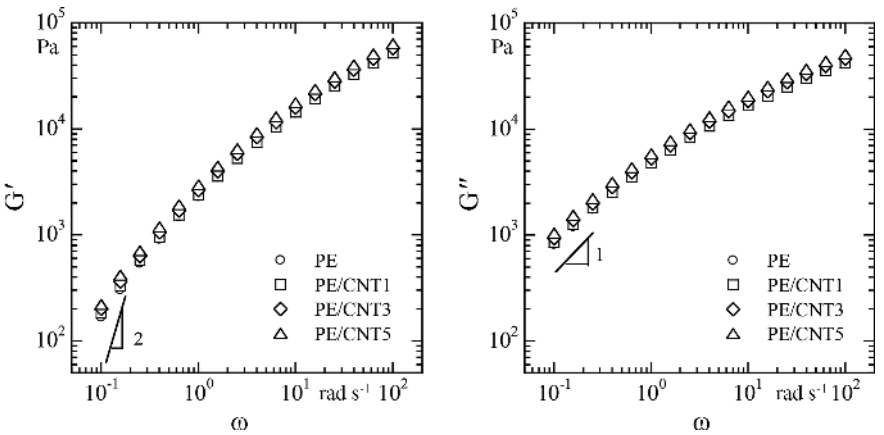

Fig. 1. Storage modulus G′ (A) and loss modulus G″ (B) as a function of angular frequency ω for PE/CNT with various CNT contents at 200 °C

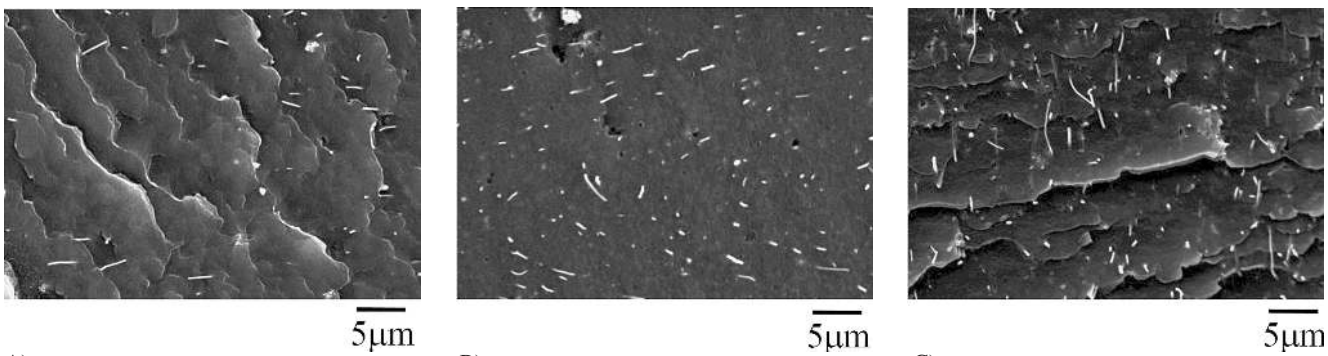

Fig. 2. Scanning electron microscopy micrographs of PE/CNT1 (A), PE/CNT3 (B) and PE/CNT5 (C)

under a shear rate of 0.01 s^{-1}. The linear elongational viscosity, which is independent of $\dot{\varepsilon}$, generally agrees with $3\eta_s^+$, a relationship known as Trouton's rule (Trouton, 1906). In other words, $3\eta_s^+$ quantifies the elongational stress growth function in the linear viscoelastic state. The η_E^+ of PE follows the linear viscoelastic function $3\eta_s^+$ over the entire time scale under low strain rates, but rapidly overtakes $3\eta_s^+$ under high strain rates. The steep increase of η_E^+ relative to $3\eta_s^+$ is known as strain hardening. That is, we state that PE exhibits strain-hardening behavior. Strain hardening typifies polymer systems containing long branched chains, because the branched chains suppress the contraction of the polymer chain during elongational deformation (Wagner et al., 2006; Sugimoto et al., 2009). This fact explains the well-known relationship between strain hardening and polymer chain extension (Bach et al., 2003; Nielsen et al., 2006). Thus, strain hardening of PE is the expected result. On the other hand, the PE/CNT5 composite also exhibits strain hardening; i.e., steep increase of η_E^+ depending on time and $\dot{\varepsilon}$. Indeed, the linear elongational viscosity of PE/CNT5 accorded with $5.4\eta^+_{s\_matrix}$, where $\eta^+_{s\_matrix}$ is the linear shear viscosity of PE, as shown in Fig. 4B. Here, the coefficient 5.4 was the value to accord to $\eta^+_{s\_matrix}$. In other words, the linear elongational viscosity of PE was specifically enhanced by the presence of CNTs.

The elongational viscosity enhancement $\eta_{E,r}$ has been discussed by the theoretical equation proposed by Batchelor (and is known as Batchelor's theory) (Batchelor, 1971). According to this theory for a semi-dilute regime, the $\eta_{E,r}$ of a polymer mixture containing anisotropic fibers is given by

$$\eta_{E,r} = \frac{\eta_E}{\eta_{s\_matrix}} - 3 = \frac{4\phi(L/d)^2}{3\ln(\pi/\phi)}. \quad (2)$$

The $\eta_{E,r}$ is attributable to fiber orientation during the elongational deformation (Mewis and Metzner, 1974; Lubansky et al., 2005). Especially, Miyazono et al. (2011) reported that Batchelor's equation is applicable to a molten polymer composite (PS/CNT), and quantitatively clarifies the orientation of fibers in a polymer matrix. Assuming a 50 % length reduction in our system, $\eta_{E,r}$ is calculated as 2.36, which is approximately consistent with the experimental data. This result suggests a significant association between the shear and elongational rheological responses for terminal relaxation behavior. On the other hand, the strain hardening of composites becomes weaker than that of the matrix as the aspect ratio of the fillers increases according to Takahashi et al. (Takahashi et al., 1999). Ferec et al. (2009) also found that the strain hardening of polypropylene was suppressed by glass fiber, irrespective of the fiber initial orientation. In order to quantify the non-linear behavior, the strain hardening parameter λ has been often used (Takahashi et al., 1999; Le Meins et al., 2003) as:

$$\lambda = \frac{\eta_E(\text{high strain rate, t})}{\eta_E(\text{low strain rate, t})} = \exp(\alpha\varepsilon*),$$
$$\varepsilon* = \varepsilon - \varepsilon_c \text{ for } \varepsilon > \varepsilon_c, \quad (3)$$

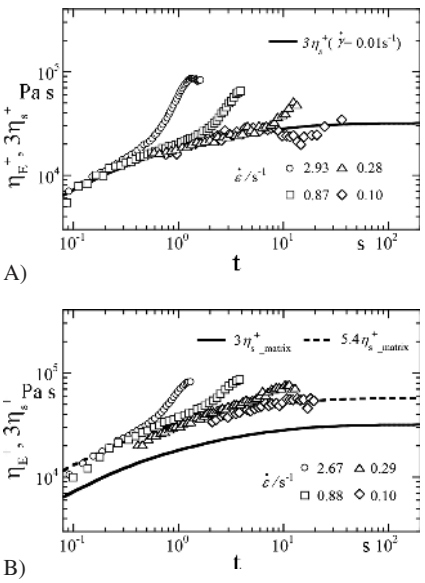

Fig. 4. Time t dependence of uniaxial elongational viscosity η_E^+ at various strain rates $\dot{\varepsilon}$ for PE (A) and PE/CNT5 (B) at 200 °C. The solid lines represent $3\eta_s^+$, where η_s is the linear shear viscosity measured with rotational rheometry

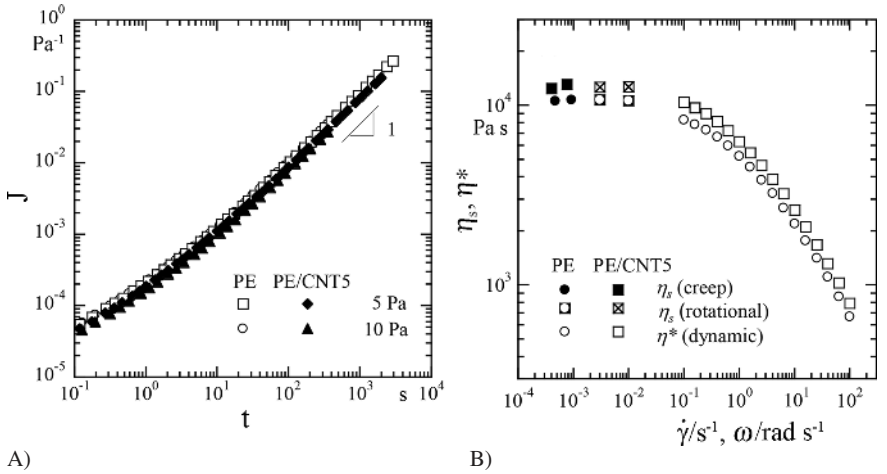

Fig. 3. Creep compliance J of PE and PE/CNT5 as a function of time t at 200 °C (A). Shear viscosity η_s as a function of strain rate $\dot{\gamma}$ for PE and PE/CNT5 at 200 °C (B). To compare with the complex viscosity η^* measured in the dynamic mode, η^* of PE and PE/CNT5 are also plotted

where α is named the strain hardening intensity. This equation was proposed on the basis of an exponential increase of η_E with a α above a critical strain ε_c (around 1) (Koyama and Ishizuka, 1983; Ninegishi et al., 2001). To confirm the effect of CNT on the extension of the chains, the relationship between the viscosity and strain is shown in Fig. 5A. Here, the exponential approximation was tried for strains above 1 because the time dependence of the linear viscosity function curves of PE and PE/CNT5 is equal. The solid and dash lines represent the fitting curves of PE and PE/CNT5, respectively. The determination coefficient, R^2, in the fitting curves fell within $0.94 \sim 0.99$. From these results, α is plotted as a function of strain rate $\dot{\varepsilon}$ in Fig. 5B. As shown in Fig. 5A, the viscosity of PE/CNT5 was larger than that of PE at $\dot{\varepsilon}$ of 0.3 s^{-1} independently of the strain. By contrast, in $\dot{\varepsilon} \geq 1\ s^{-1}$, the viscosity of PE was larger than that of PE/CNT5 above a strain of 3. The value of α decreased with the presence of CNTs at each $\dot{\varepsilon}$. Therefore, the excessive extension of chains in high strain region was suppressed with CNTs. This behavior is similar to that presented in previous reports (Takahashi et al., 1999; Le Meins et al., 2003). A plausible explanation comes from Laun (1984), who suggested that a complex flow containing shear and elongational deformation is induced between the rigid fibers on a macroscopic scale. It is suggested that the steady uniaxial elongational viscosity at high $\dot{\varepsilon}$ (observation region of strain hardening) hardly changed by the presence of CNTs although the excessive extension of chains was inhibited around the CNTs. Wherein the effect of CNTs on the normal stress difference N_1, which means the extension degree of chain in shear deformation, was investigated.

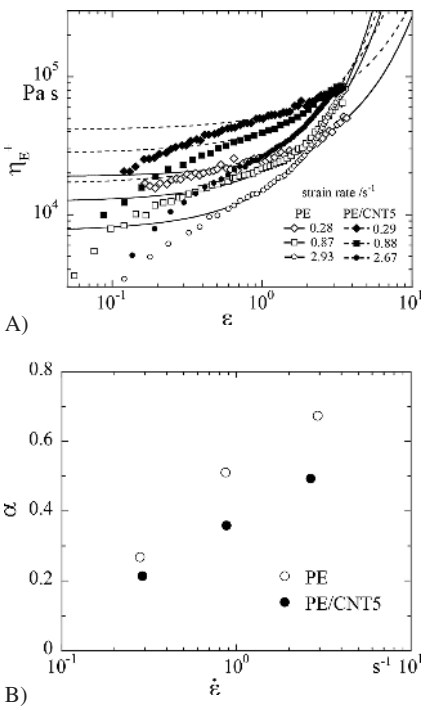

Fig. 5. Uniaxial elongational viscosity η_E^+ as a function of strain ε of PE and PE/CNT5 at 200 °C. Solid and dash lines represent the exponential approximation curve above 1 of ε of PE and PE/CNT5, respectively (A). Strain hardening intensity α as a function of strain rate $\dot{\varepsilon}$ of PE and PE/CNT5 at 200 °C (B)

The steady state value of N_1 as a function of strain rate $\dot{\gamma}$ is displayed in Fig. 6. As shown there is a very weak effect of the CNTs on the N_1 of PE. It is important to note that the extension of chains hardly changes with the presence of CNTs in shear flow although the excessive extension of chains is suppressed in elongational flow.

3.2 Capillary Extrusion Behavior

Figure 7 shows photographs of PE and PE/CNT5 extrudates passing through the die with L/D = 10 under various apparent shear rates $\dot{\gamma}_{ap}$. $\dot{\gamma}_{ap}$ was defined as the shear rate on the die wall, assuming a Newtonian fluid. Since the molten PE behaves as a non-Newtonian fluid, $\dot{\gamma}_{ap}$ and the apparent shear stress τ_{ap} require correction by the Rabinowitch and Bagley equations, respectively. The pressure drop ΔP, which is one correction coefficient, was experimentally checked with three L/D ratios of the die. The values of ΔP between the entrance and exit of the capillary die are plotted against the CNT content ϕ_w under several shear rates $\dot{\gamma}_{ap}$ in Fig. 8. As is evident in the figure, CNT addition exerts a minimal effect on the ΔP of PE. Hereafter, we investigate the effect of CNT on the swell and melt fracture

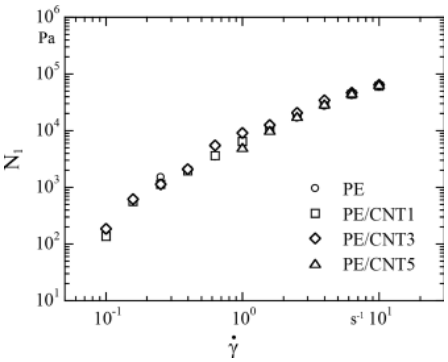

Fig. 6. Normal stress difference N_1 as a function of strain rate $\dot{\gamma}$ of PE and PE/CNT with various CNT contents at 200 °C

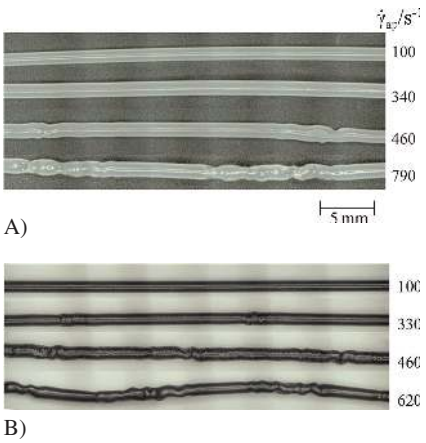

Fig. 7. Optical photographs of extruded samples of PE and PE/CNT5 using the die having L/D = 10/1 at various apparent shear rates $\dot{\gamma}_{ap}$ and 200 °C

phenomena of PE through the die with L/D = 10/1 based on the $\dot{\gamma}_{ap}$.

Figure 9 plots the swell ratio SR, defined as the diameter ratio of the extrudate to the die, as a function of $\dot{\gamma}_{ap}$ at various CNT contents. $SR_{PE/CNT}$ was lower than SR_{PE} although the swell ratios of PE and PE/CNT (denoted by SR_{PE} and $SR_{PE/CNT}$, respectively) both increased with $\dot{\gamma}_{ap}$. To confirm the volume reduction of PE on the swell ratio, Fig. 10 plots $SR_{PE/CNT}$ normalized by SR_{PE} as a function of volume fraction of CNT under specified $\dot{\gamma}_{ap}$, since the swelling of the CNT is minimal. As shown in this figure, the decrease of swell could not be explained only by the volume reduction of PE. The decrease of swell was also enhanced under higher $\dot{\gamma}_{ap}$. Thus, the swell reduction is not attributable to the reduced PE volume.

When the molten polymer emerges from the die exit, the normal stress imposed by the extension of the polymer chain is released, and the extrudate expands. In other words, the swelling phenomenon relates to the melt elasticity and is governed by the recovery of the elastic deformation imposed in the capillary. In our case, the swell of PE clearly decreased with CNT content although the N_1 of PE hardly changed irrespective of CNT content. It is likely that the recovery of the stretched chain might be suppressed at the die exit since the extension of the chain in the capillary die is not be influenced by the CNTs. Muenstedt et al. (2008) deduced the dynamics of chains in PMMA/clay composites from the creep and recoverable creep behavior of PMMA. In their report, the recoverable creep compliance increased with increasing clay content, although the creep compliance was essentially independent of the clay content. They attributed the increase in recoverable creep compliance to declined molecular mobility by enhancement of the interaction between the chains and the clay particles in the very low shear stress field. However, the recoverable creep compliance of PE was quite similar to that of PE/CNT5. This result suggested that the CNTs might not constrict the elastic recovery of PE. On the other hand, the relationship between the orientation of fibers and the flow patterns of the polymeric fluid was well investigated both experimentally and theoretically (Ausias, 1994; Chiba and Nakamura, 1998). According to these reports, it is expected that the CNTs, which become oriented in the flow direction in the capillary die, turn in a direction perpendicular to the flow direction at the capillary die exit except in the surface layer because the flow velocity in the core rapidly reduces at the die exit. If the stretched chain relaxes with turning of CNTs, the swell reduces due to contraction in the cross sectional direction. Figure 11 shows the morphology of the cross section of the extrudate at the center (A) and near the edge (B), which is at a location 100 μm away from the surface, at several shear rates. A number of long CNTs are shown at the center of the extrudate with increasing strain rate. The CNTs lined parallel to the cross section of the extrudate appear as long rods even near to the surface. The result of morphology observation leads to the presumption that the swell decreased with increasing strain rate by increasing of the orientation of the CNTs. Therefore, we conclude that the swell reduction is attributable to the orientation of CNTs induced by the deceleration at the die exit.

Finally, we discuss the effect of CNT on the melt fracture of PE. Irrespective of the CNT content, we observed three types of extrusion behavior as the volumetric flow rate is increased: stable, transition, and fracture. The relationship between the shear rate and the CNT content is presented in Fig. 12. As

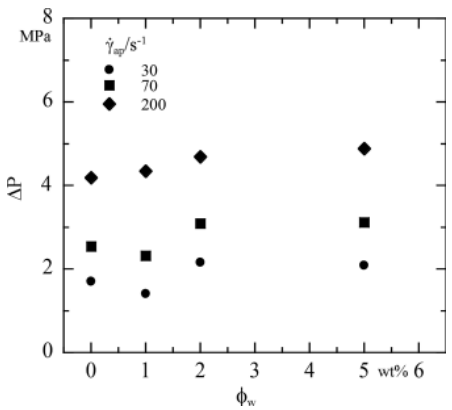

Fig. 8. Relationship between the pressure drop ΔP calculated in the capillary flow test and CNT weight content ϕ_w at several strain rates $\dot{\gamma}$ at 200°C

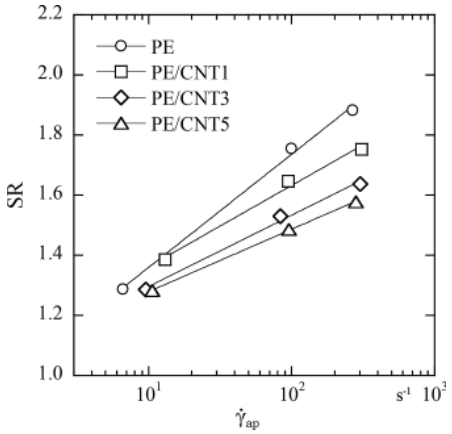

Fig. 9. Swell ratio SR, defined as the ratio of the diameter of the extrudate to that of the die, as a function of apparent strain rate $\dot{\gamma}_{ap}$ using the die having L/D = 10/1 at 200°C

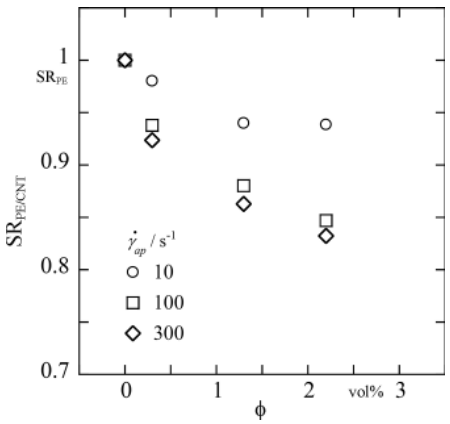

Fig. 10. Swell ratio of PE/CNT normalized by the swell ratio of PE $SR_{PE/CNT}/SR_{PE}$ as a function of the CNT volume contents ϕ in the case of the die having L/D = 10/1

shown in the diagram, CNT addition increased the likelihood of melt fracture phenomena; i. e., melt fracture was encouraged in the PE/CNT composite. Rothstein et al. reported that extensional flow (which is an accelerated flow) develops in the contraction area between the reservoir and the capillary (Rothstein and McKinley, 2001). The extensional stress at the die entrance might be reduced by a corner vortex forming at the die entrance, which grows with increasing volumetric flow rate. If the corner vortex cannot suppress the extensional stress, melt fracture may occur. According to Meller et al. (2002), melt fracture occurs above a critical extensional stress at the die entrance. If melt fracture develops above a critical extensional stress in PE, it could reasonably be promoted by the addition of CNTs, because the linear elongational viscosity increases (Fig. 4 and 5A). Moreover, it is likely that the elongational viscosity lightly enhances because CNTs are easily orientated in the flow direction in the accelerated flow (Ausias, 1994; Chiba and Nakamura, 1998). Therefore, the promotion of melt fracture is due to the orientation of CNTs at the die entrance.

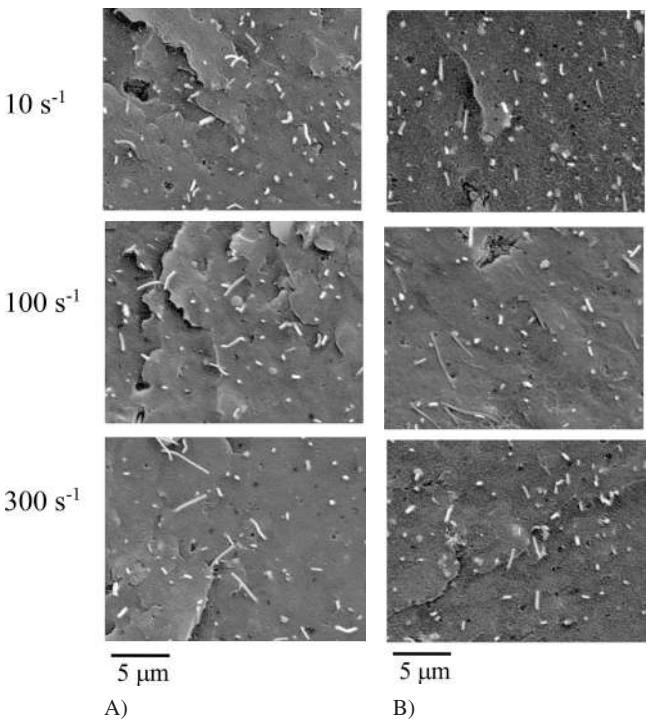

Fig. 11. Scanning electron microscopy micrographs of the cross section of extrudate of PE/CNT5 at (A) center and (B) edge, which is 100 μm away from the surface, at several strain rates

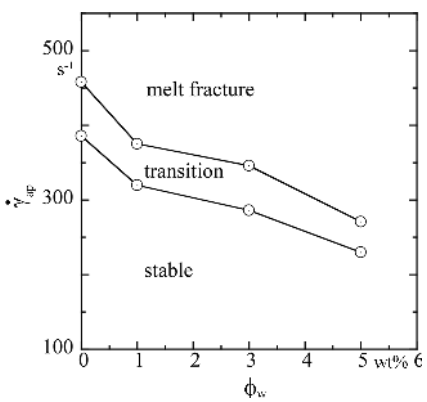

Fig. 12. Extrudate diagram showing the relationship between the apparent shear rate $\dot{\gamma}_{ap}$ and the CNT weight contents ϕ_w

4 Conclusion

We investigated the effect of CNTs on the capillary flow behavior of low-density PE, varying the CNT content from 0 to 5 wt%. CNTs were dispersed in the PE matrix and all the specimens belonged to the semi-dilute regime from the view point of SEM observation. The terminal relaxation behavior of PE hardly changed with the presence of CNTs and the shear viscosity was slightly enhanced. However, the linear elongational viscosity of PE/CNT exceeded $3\eta_s^+$, whereas that of PE coincided with $3\eta_s^+$, as expected. By considering Batchelor's theory, we inferred that the CNTs orient along the direction of elongational flow. The nonlinear behavior, which is strain hardening, of PE decreased with CNT addition, indicating the suppression of the extension of PE chains. On the other hand, the steady state normal stress difference of PE was scarcely affected by CNTs in shear deformation. As revealed by the capillary extrusion behavior, the swell ratio of the PE (which was defined as the extrudate to die diameter ratio) is a decreasing function of CNT. We attribute the reduced swelling to the orientation of CNTs induced by decelerated flow at the die exit considering SEM observations. On the other hand, melt fracture occurs under lower shear rates in PE/CNT than in PE, probably because the elongational viscosity easily enhanced due to orientation of CNTs in accelerated flow at die entrance. We summarize that the extrusion behavior drastically changes due to orientation and rearrangement of CNTs attributed to accelerated and decelerated flow in semi-dilute regime.

References

Ausias, G., Agassant, J. F. and Vincent, M., "Flow and Fiber Orientation Calculations in Reinforced Thermopastic Extruded Tubes", Int. Polym. Proc., **9**, 51 – 59 (1994), DOI:10.3139/217.940051

Bach, A., Almdal, K., Rasmussen, H. K. and Hassager, O., "Elongational Viscosity of Narrow Molar Mass Distribution Polystyrene", Macromolecules, **36**, 5174 – 5179 (2003), DOI:10.1021/ma034279q

Batchelor, G. K., "The Stress Generated in a Non-Dilute Suspension of Elongated Particles by Pure Straining Motion", J. Fluid Mech., **46**, 813 – 829 (1971), DOI:10.1017/S0022112071000879

Chen, D. Z., Yang, H. Y., He, P. S. and Zhang, W. A., "Rheological and Extrusion Behavior of Intercalated High-Impact Polystyrene/ Organomontmorillonite Nanocomposites", Compos. Sci. Technol., **65**, 1593 – 1600 (2005), DOI:10.1016/j.compscitech.2005.01.011

Chiba, K., Nakamura, K., " Numerical Solution of Fiber Suspension Flow through a Complex Channel", J. Non-Newtonian Fluid Mech., **78**, 167 – 185 (1998), DOI:10.1016/S0377-0257(98)00067-6

Cox, W. P., Merz, E. H., "Correlation of Dynamic and Steady-Flow Viscosities", J. Polym. Sci., **28**, 619 – 622 (1958), DOI:10.1002/pol.1958.1202811812

Dalir, H., Farahani, R. D., Nhim, V., Samson, B., Levesque, M. and Therriault, D., "Preparation of Highly Exfoliated Polyester-Clay Nanocomposites: Process-Property Correlations", Langmuir, **28**, 791 – 803 (2012), DOI:10.1021/la203331 h

Férec, J., Heuzey, M. C., Pérez-González, J., De Vargas, L., Ausias, G. and Carreau, P. J., "Investigation of the Rheological Properties of Short Glass Fiber-Filled Polypropylene in Extensional Flow", Rheol. Acta, **48**, 59 – 72 (2009), DOI:10.1007/s00397-008-0309-9

Goutille, Y., Majeste, J. C., Tassin, J. F., Guillet, J., "Molecular Structure and Gross Melt Fracture Triggering", J. Non-Newtonian Fluid Mech., **111**, 175 – 198 (2003), DOI:10.1016/S0377-0257(03)00054-5

Handge, U. A., Zeiler, R., Dijkstr, D. J., Meyer, H. and Altstadt, V., "On the Determination of Elastic Properties of Composites of Polycarbonate and Multi-Wall Carbon Nanotubes in The Melt", Rheol. Acta, **50**, 503 – 518 (2011), DOI:10.1007/s00397-011-0558-x

Hausnerova, B., Honkova, N., Lengalova, A., Kitano, T. and Saha, P., "Rheology and Fiber Degradation during Shear Flow of Carbon-Fiber-Reinforced Polypropylenes", Polym. Sci. Ser. A, **48**, 951 – 960 (2006), DOI:10.1134/S0965545X06090100

Kharchenko, S. B., Douglas, J. F., Obrzut, J., Grulke, E. A. and Migler, K. B., "Flow-Induced Properties of Nanotube-Filled Polymer Materials", Nat. Mater., **3**, 564 – 568 (2004), DOI:10.1038/nmat1183

Koyama, K., Ishizuka, O., " Nonlinearity in Uniaxial Elongational Viscosity at a Constant Strain Rate", Polym. Proc. Eng., **1**, 55 – 70 (1983)

Larson, R. G.: The Structure and Rheology of Complex Fluids, 1rd Edition, Oxford University Press, New York (1999)

Laun, H. M., "Orientation Effects and Rheology of Short Glass Fiber-Reinforced Thermoplastics", Coll. Polym. Sci., **262**, 257 – 269 (1984), DOI:10.1007/BF01410464

Le Meins, J. F., Moldenaers, P. and Mewis, J., "Suspensions of Monodisperse Spheres in Polymer Melts: Particle Size Effects in Extensional Flow", Rheol. Acta, **42**, 184 – 190 (2003), DOI:10.1007/s00397-002-0270-y

Lubansky, A. S., Boger, D. V. and Cooper-White, J. J., "Batchelor's Theory Extended to Elongated Cylindrical or Ellipsoidal Particles", J. Non-Newtonian Fluid Mech., **130**, 57 – 61 (2005), DOI:10.1016/j.jnnfm.2005.08.001

Ma, P. C., Siddiqui, N. A., Marom, G. and Kim, J. K., "Dispersion and Functionalization of Carbon Nanotubes for Polymer-Based Nanocomposites: A Review", Composites Part A, **41**, 1345 – 1367 (2010), DOI:10.1016/j.compositesa.2010.07.003

Meller, M., Luciani, A., Sarioglu, A. and Manson, J. A. E., "Flow through a Convergence. Part 1: Critical Conditions for Unstable Flow", Polym. Eng. Sci., **42**, 611 – 633 (2002), DOI:10.1002/pen.10976

Mewis, J., Metzner, A. B., "The Rheological Properties of Suspensions of Fibers in Newtonian Fluids Subjected to Extensional Deformations", J. Fluid. Mech., **62**, 593 – 600 (1974), DOI:10.1017/S0022112074000826

Miyazono, K., Kagarise, C. D., Koelling, K. W., Mahboob, M. and Bechtel, S. E., "Shear and Extensional Rheology and Flow-Induced Orientation of Carbon Nanofiber/Polystyrene Melt Composites", J. Appl. Polym. Sci., **119**, 1940 – 1950 (2011), DOI:10.1002/app.32923

Mu, Y., Zhao, G. "Numerical Investigation of Die Geometry Effect on LDPE Annular Extrudate Swell", J. Appl. Polym. Sci., **117**, 91 – 109 (2010), DOI:10.1002/app.31490

Muenstedt, H., Katsikis, N. and Kaschta, J., "Rheological Properties of Poly(methyl methacrylate)/Nanoclay Composites as Investigated by Creep Recovery in Shear", Macromolecules, **41**, 9777 – 9783 (2008), DOI:10.1021/ma800237x

Muksing, N., Nithitanakul, M., Grady, B. P. and Magaraphan, R., "Melt Rheology and Extrudate Swell of Organobentonite-Filled Polypropylene Nanocomposites", Polym. Test., **27**, 470 – 479 (2008), DOI:10.1016/j.polymertesting.2008.01.008

Nielsen, J. K., Rasmussen, H. K., Hassager, O. and Mckinley, G. H., "Elongational Viscosity of Monodisperse and Bidisperse Polystyrene Melts", J. Rheol., **50**, 453 – 476 (2006), DOI:10.1122/1.2206711

Nigen, S., Elkissi, N., Piau, J. M. and Sadun, S., "Velocity Field for Polymer Melts Extrusion Using Particle Image Velocimetry. Stable and Unstable Flow Regimes", J. Non-Newtonian Fluid Mech., **112**, 177 – 202 (2003), DOI:10.1016/S0377 – 0257(03)00097 – 1

Minegishi, A., Nishioka, A., Takahashi, T., Masubuchi, Y., Takimoto, J. and Koyama, K., "Uniaxial Elongational Viscosity of PS/a Small Amount of UHMW-PS Blends", Rheol. Acta, **40**, 329 – 338 (2001), DOI:10.1007/s003970100165

Nithikarnjanatharn, J., Ueda, H., Tanoue, S., Uematsu, H. and Iemoto, Y., "The Rheological Behavior and Thermal Conductivity of Melt-Compounded Polycarbonate/Vapor-Grown Carbon Fiber Composites", Polym. J., **44**, 427 – 432 (2012), DOI:10.1038/pj.2011.149

Rothstein, J. P., Mckinley, G. H., "The Axisymmetric Contraction–Expansion: The Role of Extensional Rheology on Vortex Growth Dynamics and the Enhanced Pressure Drop", J. Non-Newtonian Fluid Mech., **98**, 33 – 63 (2001), DOI:10.1016/S0377-0257(01)00094-5

Schmid, C. F., Switzer, L. H. and Klingenberg, D. J., " Simulations of Fiber Flocculation: Effects of Fiber Properties and Interfiber Friction", J. Rheol., **44**, 781 – 809 (2000), DOI:10.1122/1.551116

Sugimoto, M., Koizumi, T., Taniguchi, T., Koyama, K., Saito, K., Nonokawa, D. and Morita, T., "Melt Rheology of Hyperbranched-Polystyrene Synthesized with Multisite Macromonomer", J. Polm. Sci., Part B: Polym. Phys., **47**, 2226 – 2237 (2009), DOI:10.1002/polb.21820

Switzer, L. H., Klingenberg, D. J., "Rheology of Sheared Flexible Fiber Suspensions via Fiber-Level Simulations", J. Rheol., **47**, 759 – 778 (2003), DOI:10.1122/1.1566034

Takahashi, T., Takimoto, J. I. and Koyama, K., "Uniaxial Elongational Viscosity of Various Molten Polymer Composites", Polym. Compos., **20**, 357 – 366 (1999), DOI:10.1002/pc.10362

Tanoue, S., Iemoto, Y., "Effect of Die Gap Width on Annular Extrudates by the Annular Extrudate Swell Simulation in Steady-States", Polym. Eng. Sci., **39**, 2172 – 2180 (1999), DOI:10.1002/pen.11606

Trouton, F. T., "On the Coefficient of Viscous Traction and its Relation to that of Viscosity", Proc. R. Soc. Lond. Ser. A, Contain Pap. Math. Phys., Character, **77**, 426 – 440 (1906), DOI:10.1098/rspa.1906.0038

Uematsu, H., Horisawa, N., Horikida, T., Tanoue, S. and Iemoto Y., "Effect of Carbon Fiber on the Capillary Extrusion Behaviors of High-Density Polyethylene", Polym. J., **45**, 449 – 456 (2013), DOI:10.1038/pj.2012.167

Vega, J. F., Da Silva, Y., Vicente-Alique, E., Nunez-Ramirez, R., Trujillo, M., Arnal, M. L., Muller, A. J., Dubois, P. and Martinez-Salazar, J., " Influence of Chain Branching and Molecular Weight on Melt Rheology and Crystallization of Polyethylene/Carbon Nanotube Nanocomposites", Macromolecules, **47**, 5668 – 5681 (2014), DOI:10.1021/ma501269g

Wagner, M. H., Kheirandish, S., Stange, J. and Muenstedt, H., "Modeling Elongational Viscosity of Blends of Linear and Long-Chain Branched Polypropylenes", Rheol. Acta, **46**, 211 – 221 (2006), DOI:10.1007/s00397-006-0108-0

Wassner, E., Schmidt, M. and Muenstedt, H., "Entry Flow of a Low-Density-Polyethylene Melt into a Slit Die: An Experimental Study by Laser-Doppler Velocimetry", J. Rheol., **43**, 1339 – 1353 (1999), DOI:10.1122/1.551050

Yamaguchi, M., Todd, D. B. and Gogos, C. G., "Rheological Properties of LDPE Processed by Conventional Processing Machines", Adv. Polym. Technol., **22**, 179 – 187 (2003), DOI:10.1002/adv.10047

Acknowledgements

The authors express their thanks to Dr. Takaaki Hattori, Japan Polyethylene Corporation, for the supply of polyethylene sample and useful advice.

Date received: December 26, 2014
Date accepted: June 09, 2016

Bibliography
DOI 10.3139/217.3062
Intern. Polymer Processing
XXXII (2017) 1; page 3 – 10

ISSN 0930-777X